

# Lasers with asymmetric barrier layers: A promising type of injection lasers

Levon V Asryan<sup>1</sup>, Fedor I Zubov<sup>2</sup>, Natalia V Kryzhanovskaya<sup>2</sup>, Mikhail V Maximov<sup>2</sup>, and Alexey E Zhukov<sup>2</sup>

<sup>1</sup> Virginia Polytechnic Institute and State University, Blacksburg, VA 24061, USA

<sup>2</sup> St. Petersburg National Research Academic University of Russian Academy of Sciences, Saint Petersburg 194021, Russia

E-mail: asryan@vt.edu

## Abstract

We present an overview of our theoretical and experimental work on a novel type of semiconductor lasers – quantum well (QW) lasers with asymmetric barrier layers (ABLs). Our experimental work supports our theoretical derivations — ABL QW lasers demonstrate superior operating characteristics as compared to conventional QW lasers. In particular, the threshold current is lower and more temperature-stable, the light-current characteristic is more linear, and the wall-plug efficiency is higher in ABL lasers.

## 1. Introduction

Low lasing threshold, as well as temperature-stable and high-power operation, have always been desirable in semiconductor lasers [1]–[13]. In conventional diode lasers with a quantum-confined active region, a significant fraction of electrons and holes does not enter into the active region and thus does not contribute to stimulated recombination therein. Instead, this fraction is consumed by spontaneous recombination in the waveguide region [optical confinement layer (OCL)], wherein the carriers are initially injected from the cladding layers and which contains (in its central part) the active region [Figure 1(a)]. The parasitic electron-hole recombination outside a low-dimensional active region presents a major challenge in conventional injection lasers. Due to this recombination, the laser characteristics are adversely affected – the threshold current is increased and more temperature-sensitive and the light-current characteristic (LCC) is sublinear, even in the absence of heating effects.

To overcome the limitations placed on the operating characteristics by recombination outside the active region, novel designs of semiconductor lasers were proposed – one using double tunnelling-injection (injection of both electrons and holes) into the active region [14]–[22] and the other using asymmetric barrier layers (ABLs) [15]–[17] [one on each side of the active region – see Figure 1(b, c)]. The active region in these novel lasers can be in the form of either a single quantum well (QW) or a single layer with quantum dots.

Here we present an overview of our theoretical [23]–[27] and experimental [28]–[32] work on ABL QW lasers. Our experimental work supports our theoretical derivations — ABL QW lasers demonstrate superior operating characteristics as compared to conventional QW lasers. In particular, the threshold current is lower and more temperature-stable, the LCC is more linear, and the wall-plug efficiency is higher in ABL lasers.



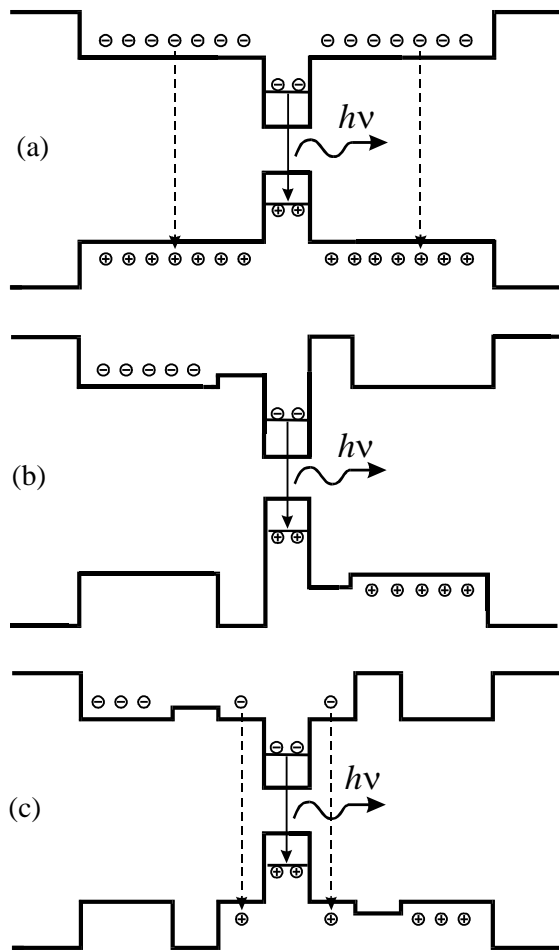


**Figure 1.** Schematic energy band diagrams of a conventional laser (a) and ABL lasers without (b) and with (c) intermediate layers. The vertical arrows show the electron-hole recombination.

## 2. ABL laser structures

Figures 1(b, c) show the schematic energy band diagrams of ABL lasers. The barrier layers are asymmetric in that they have considerably different heights for the carriers of opposite signs. The layer located on the electron- (hole-) injecting side of the structure [left- (right-) hand side in Figs. 1(b, c)] provides a low barrier (ideally no barrier) for electrons (holes) [so that it does not prevent electrons (holes) from easily approaching the active region] and a high barrier for holes (electrons) [so that holes (electrons) injected from the opposite side of the structure do not overcome it].

The use of ABLs in the structure of Figure 1(b) will thus secure that there will be no electrons and holes simultaneously (and hence no parasitic electron-hole recombination) outside the active region. In the structure of Figure 1(c), there will however be both electrons and holes (and hence some electron-hole recombination) not only in the active region but also in two intermediate layers located between the active region and each of the ABLs. The presence of these thin intermediate layers may be required in order to facilitate the flux switches during epitaxial growth process and to prevent from the active region re-evaporation [33, 34].

We discuss below the calculated and experimental characteristics of ABL QW lasers.

## 3. Threshold characteristics

The threshold current density of a QW laser is given as the sum of the current densities of spontaneous radiative recombination in and outside the QW,

$$j_{th} = j_{sp,th}^{QW} + j_{sp,th}^{outside} \quad (1)$$

The current densities of spontaneous radiative recombination in and outside the QW are

$$j_{sp,th}^{QW} = eB_{2D}n^{QW}p^{QW}, \quad (2)$$

$$j_{sp,th}^{outside} = eb^{outside}B_{3D}n_{th}^{outside}p_{th}^{outside}, \quad (3)$$

where  $e$  is the electron charge,  $B_{2D}$  is the spontaneous radiative recombination coefficient for a two-dimensional region (QW) (see [35] for the expression for  $B_{2D}$ ),  $n^{QW}$  and  $p^{QW}$  are the two-dimensional electron and hole densities in the QW,  $b^{outside}$  is the thickness of the region outside the QW wherein the parasitic electron-hole recombination occurs,  $B_{3D}$  is the spontaneous radiative recombination

coefficient for the material of that region (see [5, 35] for the expression for  $B_{3D}$ ), and  $n_{th}^{outside}$  and  $p_{th}^{outside}$  are the free electron and hole densities in that region at the lasing threshold.

In conventional QW lasers (CQWLs),  $b^{outside}$  is the thickness of the entire OCL and hence is large [300 nm in the structure of Figure 5(a)]. In the ABL QW laser with intermediate layers,  $b^{outside}$  is the sum of the thicknesses of the intermediate layers, which are very thin [5 nm each in the structure of Figure 5(b)], and hence is very small. In the ABL QW laser without intermediate layers,  $b^{outside}$  is simply zero since there is no region outside the QW wherein the electron-hole recombination occurs. Consequently, the parasitic recombination current density  $j_{spon,th}^{outside}$  is high in CQWLs, low in the ABL QW laser with intermediate layers, and zero in the ABL QW laser without intermediate layers. This is illustrated in figures 2 and 3, which show the calculated threshold current density against cavity length and temperature, respectively. As seen from the figures, the threshold current density is considerably higher in the reference CQWL as compared to both ABL QW lasers and there is no much difference between the threshold current density in the ABL QW lasers without and with intermediate layers.

The temperature dependence of threshold current in semiconductor lasers is described by the parameter  $T_0$  termed as ‘characteristic temperature’ and defined as

$$T_0 = \left( \frac{\partial \ln j_{th}}{\partial T} \right)^{-1}. \quad (4)$$

As clear from (4), the higher  $T_0$ , the more temperature-stable is  $j_{th}$ .

In CQWLs, the temperature dependence of  $j_{th}$  is primarily due to such dependence of the parasitic recombination current density in the entire OCL,  $j_{spon,th}^{outside}$ , and hence  $T_0$  is low. In the ABL QW laser without intermediate layers, the temperature dependence of  $j_{th}$  is merely due to such dependence of the recombination current density in the QW,  $j_{spon}^{QW}$ , and hence  $T_0$  is very high (ideally,  $T_0$  calculated for  $j_{spon}^{QW}$  is equal to  $T$  – see [23]). In the ABL QW laser with intermediate layers, the temperature dependence of  $j_{th}$  is due to such dependence of both recombination current densities in and outside the QW. For the cavity lengths considerably exceeding the shortest cavity length (the minimum tolerable cavity length below which the lasing is impossible to attain – see [36]), the contribution of the parasitic recombination in the intermediate layers is small and hence  $T_0$  is high also in this ABL QW laser [23]. This is illustrated in Figure 4, which shows the calculated  $T_0$  against cavity.

Figures 6 and 7 show the threshold characteristics measured in our experimental ABL QW laser structure with intermediate layers [the structure of Figure 5(b)] –  $T_0$  against reciprocal cavity length, and  $T_0$  and  $j_{th}$  against temperature. For comparison, the characteristics measured for the reference CQWL structure [the structure of Figure 5(a)] are also presented. As seen from the figures,  $T_0$  is considerably higher in the ABL QW laser as compared to the reference CQWL. In particular, at the operating temperature 20 °C,  $T_0$  is 143 K in the ABL QW laser while it is 99 K in the reference CQWL.

#### 4. Power characteristics

The LCC of a diode laser (the output optical power  $P$  versus injection current density  $j$ ) is given by

$$P(j) = \frac{\hbar\omega}{e} S (j - j_{th}) \eta_{int}(j), \quad (5)$$

where  $\hbar\omega$  is the photon energy,  $S = WL$  is the cross-section of the junction,  $W$  is the lateral size of the device,  $L$  is the cavity length, and  $\eta_{int}(j)$  is the internal differential quantum efficiency (efficiency of stimulated recombination).

In the CQWL, the internal quantum efficiency is a decreasing function of the injection density. The following expression was derived for  $\eta_{int}$  in [37]–[39]:

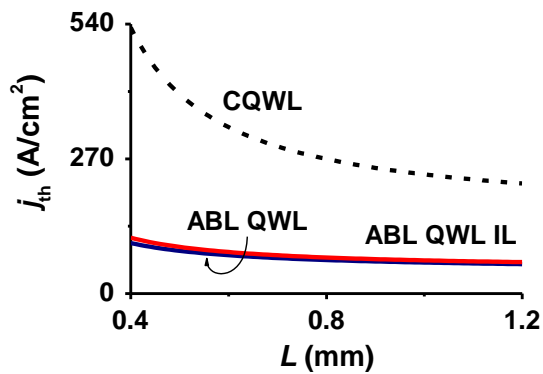


**Figure 2.** Threshold current density vs. cavity length in the ABL QW lasers without and with intermediate layers and reference conventional quantum well laser (CQWL).

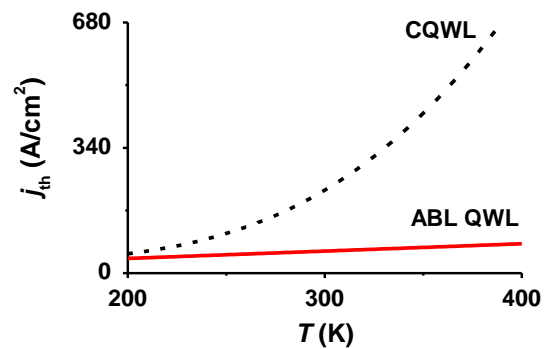


**Figure 3.** Threshold current density vs. temperature in the ABL QW laser without intermediate layers and reference CQWL.

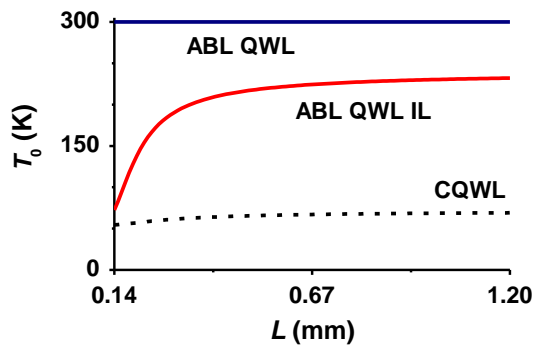


**Figure 4.** Characteristic temperature vs. cavity length in the ABL QW lasers without and with intermediate layers and reference CQWL.

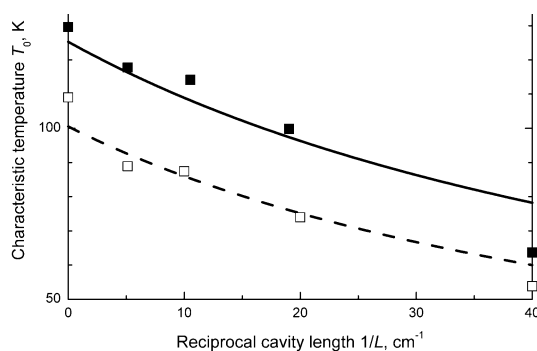


**Figure 6.** Experimental (symbols) and calculated (curves) dependences of the characteristic temperature on the reciprocal cavity length in the ABL QW laser with intermediate layers (solid curve, dark squares) and reference CQWL (dashed curve, open squares).

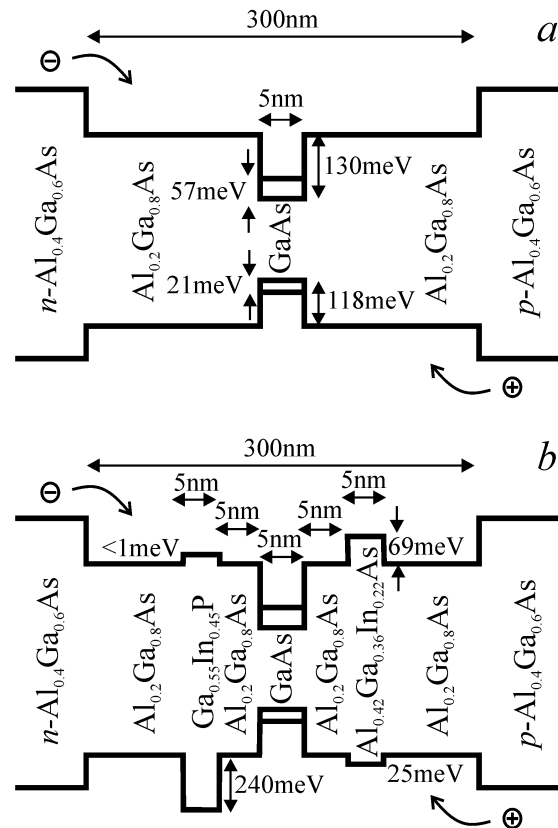


**Figure 5.** Energy band diagrams of the experimental structures: (a) reference CQWL and (b) ABL QW laser with intermediate layers. The lasing wavelength at 20°C is 833.8 nm in the CQWL and 835.6 nm in the ABL QW laser.

$$\eta_{\text{int}}(j) = \left[ \frac{1}{2} + \frac{j_{\text{spn, th}}^{\text{outside}}}{\langle j_{\text{capt, th}} \rangle_{\text{harmon}}} + \sqrt{\left( \frac{1}{2} + \frac{j_{\text{spn, th}}^{\text{outside}}}{\langle j_{\text{capt, th}} \rangle_{\text{harmon}}} \right)^2 + \frac{j_{\text{spn, th}}^{\text{outside}}}{\langle j_{\text{capt, th}} \rangle_{\text{geom}}} \frac{j - j_{\text{th}}}{\langle j_{\text{capt, th}} \rangle_{\text{geom}}}} \right]^{-1}, \quad (6)$$

where  $\langle j_{\text{capt, th}} \rangle_{\text{harmon}}$  and  $\langle j_{\text{capt, th}} \rangle_{\text{geom}}$  are the harmonic and geometric means of the current densities  $j_{\text{capt, n, th}}$  and  $j_{\text{capt, p, th}}$  of electron and hole capture into the QW at the lasing threshold,

$$\frac{1}{\langle j_{\text{capt, th}} \rangle_{\text{harmon}}} = \frac{1}{2} \left( \frac{1}{j_{\text{capt, n, th}}} + \frac{1}{j_{\text{capt, p, th}}} \right), \quad (7)$$

$$\langle j_{\text{capt, th}} \rangle_{\text{geom}} = \sqrt{j_{\text{capt, n, th}} j_{\text{capt, p, th}}}. \quad (8)$$

As seen from (6), the higher the parasitic recombination current density at the lasing threshold,  $j_{\text{spn, th}}^{\text{outside}}$ , the stronger the decrease in  $\eta_{\text{int}}$  with increasing  $j$ . Hence,  $\eta_{\text{int}}$  decreases considerably with  $j$  and the LCC is strongly sublinear in the CQWL. As already mentioned above,  $j_{\text{spn, th}}^{\text{outside}}$  is very low in the ABL QW laser with intermediate layers and simply zero in the ABL QW laser without intermediate layers. Hence,  $\eta_{\text{int}}$  decreases only slightly with increasing  $j$  in the ABL QW laser with intermediate layers and constant (unity) in the ABL QW laser without intermediate layers; consequently, the LCC is just slightly sublinear in the ABL QW laser with intermediate layers and virtually linear in the ABL QW laser without intermediate layers. This is illustrated in Figures 8-10, which present the following characteristics calculated as functions of the injection current: the parasitic recombination current outside the QW, the internal differential quantum efficiency, and the LCC.

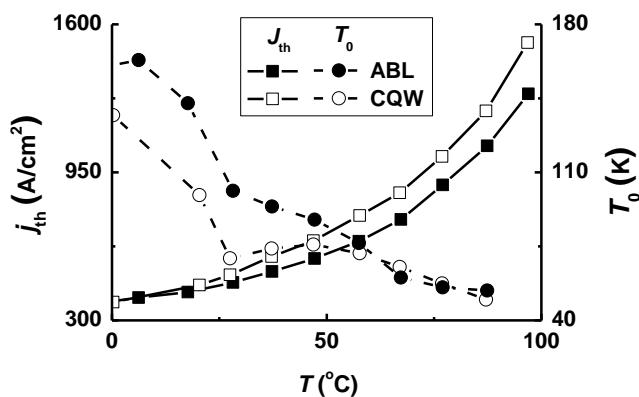


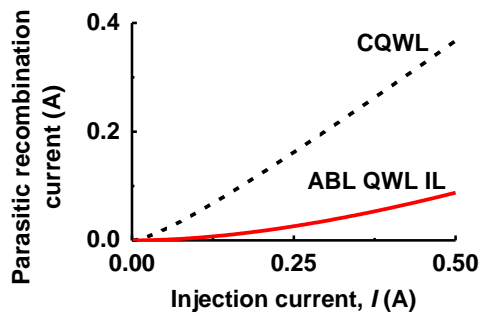
**Figure 7.** Experimental threshold current density (squares, left axis) and characteristic temperature (circles, right axis) vs. temperature: dark symbols – ABL QW laser with intermediate layers, open symbols – reference CQWL. The cavity length is 0.5 mm.

## 5. Conclusions

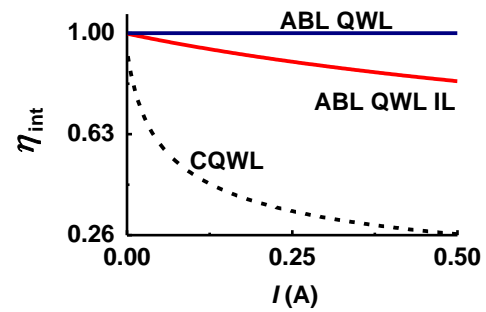
We have presented an overview of our theoretical and experimental work on a novel type of semiconductor lasers – quantum well (QW) lasers with asymmetric barrier layers (ABLs). Our experimental work supports our theoretical derivations — ABL QW lasers demonstrate superior operating characteristics as compared to conventional QW lasers. In particular, the threshold current is lower and more temperature-stable, the LCC is more linear, and the wall-plug efficiency is higher in ABL lasers.

Figure 12 shows the experimental LCC in the ABL QW laser and reference CQWL of Figure 11. As seen from Figure 12, at both operating temperatures 20 and 60 °C, the LCC is more linear and the output power is higher in the ABL laser.

Figure 13 shows the experimental wall-plug efficiency in the ABL QW laser with intermediate layers and reference CQWL of Figure 5. As seen from Figure 13, at both operating temperatures 20 and 75 °C, the efficiency is distinctly higher in the ABL laser.



**Figure 8.** Parasitic recombination current vs. injection current in the ABL QW laser with intermediate layers and reference CQWL.



**Figure 9.** Internal differential quantum efficiency vs. injection current in the ABL QW lasers without and with intermediate layers and reference CQWL.

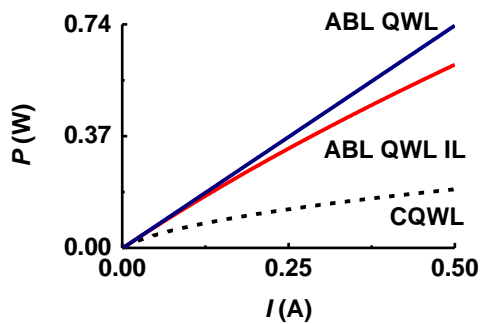


**Figure 10.** Light-current characteristic in the ABL QW lasers without and with intermediate layers and reference CQWL.

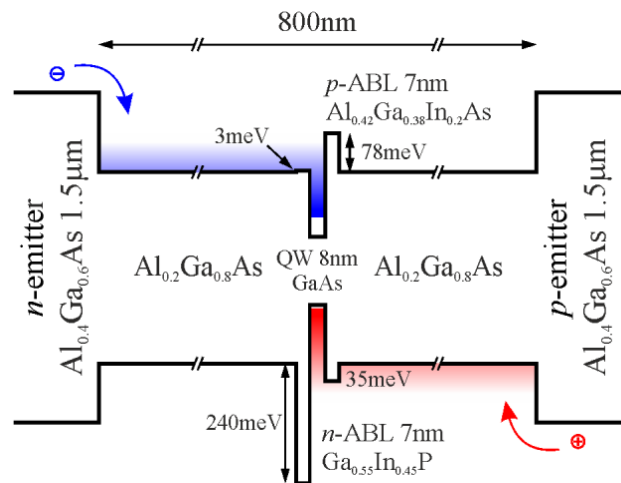


**Figure 11.** Energy band diagram of the experimental ABL QW laser used for the measurements in Figure 12.

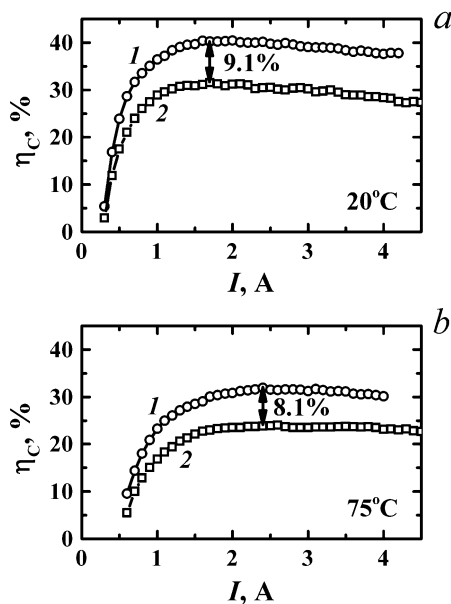


**Figure 13.** Experimental wall-plug efficiency vs. injection current in (1) the ABL QW laser with intermediate layers and (2) reference CQWL of Figure 5 at (a) 20 and (b) 75°C.

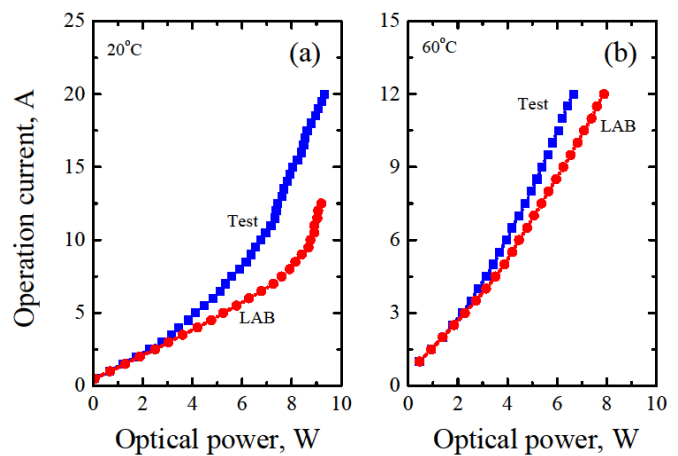


**Figure 12.** Operating current vs. output optical power measured in the ABL QW laser of Figure 11 and CQWL at 20°C (a) and 60°C (b).

## Acknowledgment

This work was supported by the Russian Science Foundation (project 14-42-00006 “A novel type of diode lasers with characteristics improved by using asymmetric barriers”).

## References

- [1] Agrawal G P and Dutta N K 1986 *Long-Wavelength Semiconductor Lasers* (New York: Van Nostrand)
- [2] Zory P S Jr ed 1993 *Quantum Well Lasers* (Boston: Academic)
- [3] Kapon E ed 1999 *Semiconductor Lasers I: Fundamentals*, 1st Edition (New York: Academic)
- [4] Temkin H, Coblenz D, Logan R A, Vandenberg J M, Yadavish R D and Sergent A M 1994 Strained quaternary quantum well lasers for high temperature operation *Appl. Phys. Lett.* **63** 2321-3
- [5] Asryan L V and Suris R A 1996 Inhomogeneous line broadening and the threshold current density of a semiconductor quantum dot laser *Semicond. Sci. Technol.* **11** 554-67
- [6] Seki S, Oohashi H, Sugiura H, Hirono T and Yokoyama K 1996 Study on the dominant mechanisms for the temperature sensitivity of threshold current in 1.3  $\mu\text{m}$  InP-based strained-layer quantum-well lasers *IEEE J. Quantum Electron.* **32** 1478-95
- [7] Kazarinov R F and Shtengel G E 1997 Effect of carrier heating on static linearity of MQW InGaAsP/InP lasers *J. Lightw. Technol.* **15** 2284-6
- [8] Maximov M V, Asryan L V, Shernyakov Y M, Tsatsul'nikov A F, Kaiander I N, Nikolaev V V, Kovsh A R, Mikhrin S S, Ustinov V M, Zhukov A E, Alferov Z I, Ledentsov N N and Bimberg D 2001 Gain and threshold characteristics of long wavelength lasers based on InAs/GaAs quantum dots formed by activated alloy phase separation *IEEE J. Quantum Electron.* **37** 676-83
- [9] Mawst L J, Bhattacharya A, Lopez J, Botez D, Garbuzov D Z, DeMarco L, Connolly J C, Jansen M, Fang F and Nabiev R F 1996 8 W continuous wave front-facet power from broad-waveguide Al-free 980 nm diode lasers *Appl. Phys. Lett.* **69** 1532-4
- [10] Garbuzov D, Xu L, Forrest S R, Martinelli R and Connolly J C 1996 1.5  $\mu\text{m}$  wavelength, SCH-MQW InGaAsP/InP broadened-waveguide laser diodes with low internal loss and high output power *Electron. Lett.* **32** 1717-9
- [11] Al-Muhanna A, Mawst L J, Botez D, Garbuzov D Z, Martinelli R U and Connolly J C 1998 High-power (>10 W) continuous-wave operation from 100- $\mu\text{m}$ -aperture 0.97- $\mu\text{m}$ -emitting Al-free diode lasers *Appl. Phys. Lett.* **73** 1182-4
- [12] Livshits D A, Kochnev I V, Lantratov V M, Ledentsov N N, Nalyot T A, Tarasov I S and Alferov Z I 2000 Improved catastrophic optical mirror damage level in InGaAs/AlGaAs laser diodes *Electron. Lett.* **36** 1848-9
- [13] Vinokurov D A, Zorina S A, Kapitonov V A, Murashova A V, Nikolaev D N, Stankevich A L, Khomylev M A, Shamakhov V V, Leshko A Yu, Lyutetskiy A V, Nalyot T A, Pikhtin N A, Slipchenko S O, Sokolova Z N, Fetisova N V and Tarasov I S 2005 High-power laser diodes based on asymmetric separate-confinement heterostructures *Semicond.*, **39** 370-3
- [14] Asryan L V and Luryi S 2001 Tunneling-injection quantum-dot laser: Ultrahigh temperature stability *IEEE J. Quantum Electron.* **37** 905-10
- [15] Asryan L V and Luryi S 2003 Temperature-insensitive semiconductor quantum dot laser *Solid-State Electron.* **47** 205-12
- [16] Asryan L V and Luryi S 2004 Quantum dot lasers: Theoretical overview *Semiconductor Nanostructures for Optoelectronic Applications* (Boston: Artech House Publishers) (pp 113-58), chapter 4
- [17] Asryan L V and Luryi S 2005 Semiconductor laser with reduced temperature sensitivity *U.S. Patent 6 870 178 B2*
- [18] Han D-S and Asryan L V 2008 Tunneling-injection of electrons and holes into quantum dots: A tool for high-power lasing *Appl. Phys. Lett.* **92** 251113

- [19] Han D-S and Asryan L V 2008 Characteristic temperature of a tunneling-injection quantum dot laser: Effect of out-tunneling from quantum dots *Solid-State Electron.* **52** 1674-9
- [20] Han D-S and Asryan L V 2009 Effect of the wetting layer on the output power of a double tunneling-injection quantum-dot laser *J. Lightw. Technol.* **27** 5775-82
- [21] Han D-S and Asryan L V 2010 Output power of a double tunneling-injection quantum dot laser *Nanotechnology* **21** 015201
- [22] Asryan L V 2015 Modulation bandwidth of a double tunnelling-injection quantum dot laser *Semicond. Sci. Technol.* **30** 035022
- [23] Asryan L V, Kryzhanovskaya N V, Maximov M V, Egorov A Yu and Zhukov A E 2011 Bandedge-engineered quantum well laser *Semicond. Sci. Technol.* **26** 055025
- [24] Zhukov A E, Kryzhanovskaya N V, Maximov M V, Egorov A Yu, Pavlov M M, Zubov F I and Asryan L V 2011 Semiconductor lasers with asymmetric barrier layers: An approach to high temperature stability *Semicond.* **45** 530-5
- [25] Asryan L V, Kryzhanovskaya N V, Maximov M V, Zubov F I and Zhukov A E 2013 Light-current characteristic of a quantum well laser with asymmetric barrier layers *J. Appl. Phys.* **114** 143103
- [26] Zhukov A E, Asryan L V, Semenova E S, Zubov F I, Kryzhanovskaya N V and Maximov M V 2015 On the optimization of asymmetric barrier layers in InAlGaAs/AlGaAs laser heterostructures on GaAs substrates *Semicond.* **49** 935-8
- [27] Asryan L V, Zubov F I, Kryzhanovskaya N V, Maximov M V and Zhukov A E 2016 Theory of power characteristics of lasers with asymmetric barrier layers: Inclusion of asymmetry in electron and hole states filling *Semicond.* **50**
- [28] Zhukov A E, Kryzhanovskaya N V, Zubov F I, Shernyakov Y M, Maximov M V, Semenova E S, Yvind K and Asryan L V 2012 Improvement of temperature-stability in a quantum well laser with asymmetric barrier layers *Appl. Phys. Lett.* **100** 021107
- [29] Zhukov A E, Asryan L V, Shernyakov Yu M, Maximov M V, Zubov F I, Kryzhanovskaya N V, Yvind K and Semenova E S 2012 Effect of asymmetric barrier layers in the waveguide region on the temperature characteristics of quantum-well lasers *Semicond.* **46** 1027-31
- [30] Zubov F I, Zhukov A E, Shernyakov Yu M, Maximov M V, Kryzhanovskaya N V, Yvind K, Semenova E S and Asryan L V 2015 The effect of asymmetric barrier layers in the waveguide region on power characteristics of QW lasers *Technical Phys. Lett.* **41** 439-42
- [31] Zubov F I, Maximov M V, Shernyakov Yu M, Kryzhanovskaya N V, Semenova E S, Yvind K, Asryan L V and Zhukov A E 2015 Suppression of sublinearity of light-current curve in 850 nm quantum well laser with asymmetric barrier layers *Electron. Lett.* **51** 1106-8
- [32] Zubov F I, Zhukov A E, Shernyakov Yu M, Maximov M V, Semenova E S and Asryan L V 2015 Diode lasers with asymmetric barriers for 850 nm spectral range: experimental studies of power characteristics *J. Phys. Conf. Ser.* **643** 012042
- [33] Zhukov A E, Kovsh A R, Egorov A Yu, Maleev N A, Ustinov V M, Volovik B V, Maximov M V, Tsatsul'nikov A F, Ledentsov N N, Shernyakov Yu M, Lunev A V, Musikhin Yu G, Bert N A, Kop'ev P S and Alferov Zh I 1999 Photo- and electroluminescence in the 1.3- $\mu\text{m}$  range from quantum-dot structures grown on GaAs substrates *Semicond.* **33** 153-6
- [34] Ledentsov N N, Kovsh A R, Shchukin V A, Mikhlin S S, Krestnikov I L, Kozhukhov A V, Karachinsky L Y, Maximov M V, Novikov I I, Shernyakov Yu M, Soshnikov I P, Zhukov A E, Musikhin Yu G, Ustinov V M, Zakharov N D, Werner P, Kettler T, Posilovic K, Bimberg D, Hu M, Nguyen H K, Song K, and Zah C-E 2006 1.3-1.5  $\mu\text{m}$  quantum dot lasers on foreign substrates: growth using defect reduction technique, high-power CW operation, and degradation resistance *Proc. SPIE* **6133** 61330S-1-12
- [35] Asryan L V 2005 Spontaneous radiative recombination and nonradiative Auger recombination in quantum-confined heterostructures *Quantum Electron.* **35** 1117-20
- [36] Asryan L V and Suris R A 1999 Spatial hole burning and multimode generation threshold in quantum-dot lasers *Appl. Phys. Lett.* **74** 1215-7



- [37] Asryan L V, Luryi S and Suris R A 2002 Intrinsic nonlinearity of the light-current characteristic of semiconductor lasers with a quantum-confined active region *Appl. Phys. Lett.* **81** 2154-6
- [38] Asryan L V, Luryi S and Suris R A 2003 Internal efficiency of semiconductor lasers with a quantum-confined active region *IEEE J. Quantum Electron.* **39** 404-18
- [39] Asryan L V and Sokolova Z N 2014 Optical power of semiconductor lasers with a low-dimensional active region *J. Appl. Phys.* **115** 023107